

Notoginsenoside R1 attenuates breast cancer progression by targeting *CCND2* and *YBX3*

Hai-Long Qin¹, Xue-Jun Wang¹, Bi-Xian Yang², Bin Du², Xue-Lin Yun¹

¹College of Pharmacy, Guizhou University of Traditional Chinese Medicine, Guiyang, Guizhou 550000, China;

²College of Food and Pharmacy Engineering, Guiyang University, Guiyang, Guizhou 550000, China.

Abstract

Background: Breast cancer (BC) is a common malignancy with highly female incidence. So far the function of notoginsenoside R1 (NGR1), the extract from *Panax notoginseng*, has not been clearly elucidated in BC.

Methods: Optimal culture concentration and time of NGR1 were investigated by cell counting kit-8 assay. Cell proliferation ability was measured by colony formation assays. Transwell assay was used to detect the effect of NGR1 on cell migration and invasion. The apoptosis rate of cells between each group was measured by TUNEL assay.

Results: NGR1 treatment has an inhibitory effect on proliferation, migration, invasion, and angiogenesis and a stimulating effect on cell cycle arrest and apoptosis of Michigan Cancer Foundation-7 (MCF-7) cells. The 50% growth inhibitory concentration for MCF-7 cells at 24 h was 148.9 mmol/L. The proportions of MCF-7 cells arrested in the G0/G1 phase were 36.94±6.78%, 45.06±5.60%, and 59.46±5.60% in the control group, 75, and 150 mmol/L groups, respectively. Furthermore, we revealed that NGR1 treatment attenuates BC progression by targeted downregulating *CCND2* and *YBX3* genes. Additionally, *YBX3* activates phosphatidylinositol 3-phosphate kinase (PI3K)/protein kinase B (Akt) signaling pathway by activating kirsten rat sarcoma viral oncogene, which is an activator of the PI3K/Akt signaling pathway.

Conclusion: These results suggest that NGR1 can act as an efficacious drug candidate that targets the *YBX3*/PI3K/Akt axis in patients with BC.

Keywords: Breast cancer; Notoginsenoside R1; *CCND2*; *YBX3*

Introduction

The incidence of breast cancer (BC), the most common neoplasm in women, is rapidly increasing worldwide, with approximately 1.7 million new cases each year.^[1,2] Nevertheless, for women with established diagnoses, survival rates have improved, but the median survival is dramatically low.^[3,4] Most metastatic or relapsed breast tumors are incurable, and substantial improvement in survival rates still remains a researchers' dream.^[5,6] BC carcinogenesis is a complex biological process, and the mechanism of BC occurrence and metastasis, even therapy, remains unclear and requires deep exploration.^[7]

Notoginsenoside R1 (NGR1), the main effective component isolated from *Panax notoginseng*, is one of the most valuable traditional Chinese medicines and was once used in ancient China to treat cardiovascular diseases. It has been well characterized by various studies and has many

pharmacological effects, including anti-inflammatory, anti-oxidant, anti-apoptotic, and anti-tumor effects.^[8-12] Regarding its anti-tumor functions, recently, investigators determined that *P. notoginseng* suppressed the metastasis of colorectal cancer (CRC) by inhibiting migration, invasion, and adhesion abilities.^[13] In addition, NGR1, one of the most important components of *P. notoginseng*, also significantly suppressed the metastasis of CRC through the regulation of matrix metalloproteinase-9, integrin-1, E-selectin, and intercellular cell adhesion molecule-1 expression. Factors of NGR1 influencing cancer prevention and treatment have also been explored in colon cancer, leukemia, and melanoma.^[14-16] However, previous studies have not addressed the effects of NGR1 on BC, and the related regulatory mechanisms remain unclear.

Migration and invasion play significant roles in tumor metastasis.^[17] With initial cancer tissue growth, the original cancer cells must separate from the primary tumor mass by losing their cell-cell contact and must

Access this article online

Quick Response Code:



Website:

www.cmj.org

DOI:

10.1097/CM9.0000000000001328

Correspondence to: Xue-Lin Yun, College of Pharmacy, Guizhou University of Traditional Chinese Medicine, Guiyang, Guizhou 550000, China
E-Mail: xuelin7532@163.com

Copyright © 2021 The Chinese Medical Association, produced by Wolters Kluwer, Inc. under the CC-BY-NC-ND license. This is an open access article distributed under the terms of the Creative Commons Attribution-Non Commercial-No Derivatives License 4.0 (CCBY-NC-ND), where it is permissible to download and share the work provided it is properly cited. The work cannot be changed in any way or used commercially without permission from the journal.

Chinese Medical Journal 2021;134(5)

Received: 22-10-2020 Edited by: Li-Shao Guo

invade the stroma. This process is called an invasion. Another specific ability of tumor cells is to produce substances that promote angiogenesis, which provide nutrition for tumor cell growth and development. Apoptosis refers to programmed cell death that occurs in normal cells without any outside attack. An increasing number of people are studying effective ways to induce or promote cancer cell apoptosis to reduce cancer.^[18,19]

In this study, we reported that NGR1 suppressed the progression of BC by inhibiting the migration, invasion, and angiogenesis of MCF-7 and MDA-MB-231 cells and promoting the apoptosis of BC cells. Furthermore, mechanistic investigations showed that NGR1 influenced BC cells by downregulating *CCND2* and *YBX3*. However, both *CCND2* and *YBX3* are recognized as oncogenes that have previously been observed in colon cancer, lung cancer, and ovarian cancer.^[12,20-25] In this study, we found that *YBX3* acts as an oncogene by activating the KRAS/phosphatidylinositol 3-phosphate kinase (PI3K)/protein kinase B (Akt) signaling pathway in MCF-7 cells. Thus, we indicated that NGR1 attenuates BC progression by targeting *CCND2* and *YBX3*; of note, *YBX3* is an activator of the KRAS/PI3K/AKT signaling pathway.

Methods

Bioinformatics analysis

Microarray datasets from the Gene Expression Omnibus (GEO) database were used to test differential expression genes after NGR1 (MedChemExpress, New Jersey, USA) treatment in BC cells. Raw microarray data were downloaded from GEO including GSE85871. Then, the raw microarray data were normalized and z-score-transformed using RMAExpress (<http://www.rmaexpress.bmbolstad.com/>).

Cell culture

MCF-7 cells, MDA-MB-231 cells, and human umbilical vein endothelial cells (HUVECs) were obtained from European Collection of Authenticated Cell Cultures (Shanghai, China). Cells were cultured in Dulbecco's modification of Eagle's medium (Gibco, Grand Island, NY, USA) supplemented with 10% heat-inactivated fetal bovine serum (FBS) (Gibco). All cells were incubated at 37°C in a 5% CO₂ humidified incubator.

Cell transfection

Small interfering RNA, si-YBX3, and si-NC were purchased from RiboBio (Guangzhou, China). The cells were seeded into six-well plates. Lipofectamine 2000 (Invitrogen, Carlsbad, CA, USA) was used to transfect MCF-7 cells according to the manufacturer's instructions.

Cell viability assay

Cells were digested by trypsin and uniformly seeded in a 96-well plate. Each group contained three duplicate wells. The wells on the edges of the 96-well plate were filled with phosphate buffer saline (PBS), and the plate was placed in a

37°C, 5% CO₂ incubator. A total of 5×10^3 cells were inoculated in each well. The medium was aspirated, and the cells were treated with a medium containing the specified concentrations of the substance for the specified durations. The cell counting kit-8 solution was added at 10 μ L/well. The 96-well plate was incubated in a 37°C incubator for 1 h. The optical density of each well at 490 nm was measured with a microplate reader. The optical density values were averaged, and the experiment was repeated at least 3 times.

Colony formation assay

A total of 1000 cells were plated in a six-well plate and mixed well with 3 mL of medium containing 10% FBS. Cells were maintained in an incubator at 37°C and 5% CO₂ for 1 week. Cells in the wells were fixed using paraformaldehyde for 30 min and were then stained with 0.1% crystal violet. Clusters containing >30 cells were counted as a single colony.

Cell migration and invasion assays

Cells were harvested, resuspended in serum-free medium, and seeded in the upper chamber of a Transwell insert containing a membrane filter (Corning, NY, USA). Medium containing 10% FBS was added to the lower chamber. The cells were incubated for 24 h. After treatment with paraformaldehyde, cells were stained with 0.1% crystal violet. Finally, cells were imaged and counted using an Olympus microscope (Tokyo, Japan).

Endothelial tube formation assay

Matrigel (Corning) (10 μ L) was added to each well of a 96-well plate and allowed to solidify (at 37°C for 30 min). HUVECs were resuspended in supernatant collected from each group. Then, 300 μ L of supernatant containing 4×10^4 HUVECs was added to each well and incubated at 37°C. After 8 h, tube formation was observed under a microscope.

Chromatin immunoprecipitation-seq (ChIP-seq)

To identify the promoter that binds to *YBX3*, a ChIP assay was performed using the EZ-Magna ChIP kit (Millipore, Shanghai, China) according to the manufacturer's protocol. In brief, cells were fixed with 4% paraformaldehyde and incubated with glycine for 10 min to generate DNA-protein cross-links. Then, the cells were lysed with Cell Lysis Buffer and Nuclear Lysis Buffer and sonicated to generate chromatin fragments of 400 to 800 bp. ChIP-qPCR and ChIP-seq of MCF-7 cells were performed using an anti-YBX3 antibody (Invitrogen). The primers are as follows: F-5'-GCCACTGATGATCTGGGAGT-3'; R-3'-GTGAAAGACAGGGAAGGGGA-5'.

Western blotting analysis

The nuclear protein fraction and total protein were prepared with an isolation kit (KeyGen Biotech, Nanjing, China). Western blotting was performed with antibodies against *CCND2*, *YBX3*, cleaved caspase-3, and cleaved

caspase-9 (Abcam Cambridge, MA, USA); glyceraldehyde-3-phosphate dehydrogenase and Bax (ProteinTech, Wuhan, China); and P-PI3K, P-AKT, and KRAS (Affinity, Biosciences OH, USA). Protein quantification was performed using ImageJ software (National Institutes of Health, Bethesda, MD, USA) and normalized to glyceraldehyde-3-phosphate dehydrogenase values.

Flow cytometric analysis of the cell cycle

The cell cycle was analyzed using flow cytometry. MCF-7 cells after treatment were digested with trypsin, washed twice with cold PBS, and centrifuged at 1000 r/min for 5 min at room temperature. Then, the cells were fixed in 70% pre-cooled ethanol at 4°C overnight, washed, and resuspended in cold PBS after fixation. For cell cycle analysis, cells were incubated in PBS containing 100 µg/mL ribonuclease for 20 min and stained with 1 mg/mL propidium iodide (Sigma, St. Louis, MO, USA) solution for 30 min at 4°C in the dark. Data were acquired using

a FACScan flow cytometer (BD, Franklin Lakes, NJ, USA).

TUNEL assay

The TUNEL assay for apoptotic cell detection was performed using an *in situ* apoptosis detection kit (Roche, Branchburg, NJ, USA) in tumor tissue sections. Apoptotic cells nine random fields per slide were identified and analyzed under a light microscope.

Statistical analysis

The results are presented as the mean ± standard deviation from three independent experiments performed in triplicate. The *P* values were calculated using Student's *t* test or one-way analysis of variance. A *P* value of <0.05 was considered to indicate a statistically significant result. Statistical analyses were performed using GraphPad Prism 6.0 statistical software (GraphPad Software Inc., La Jolla, CA, USA).

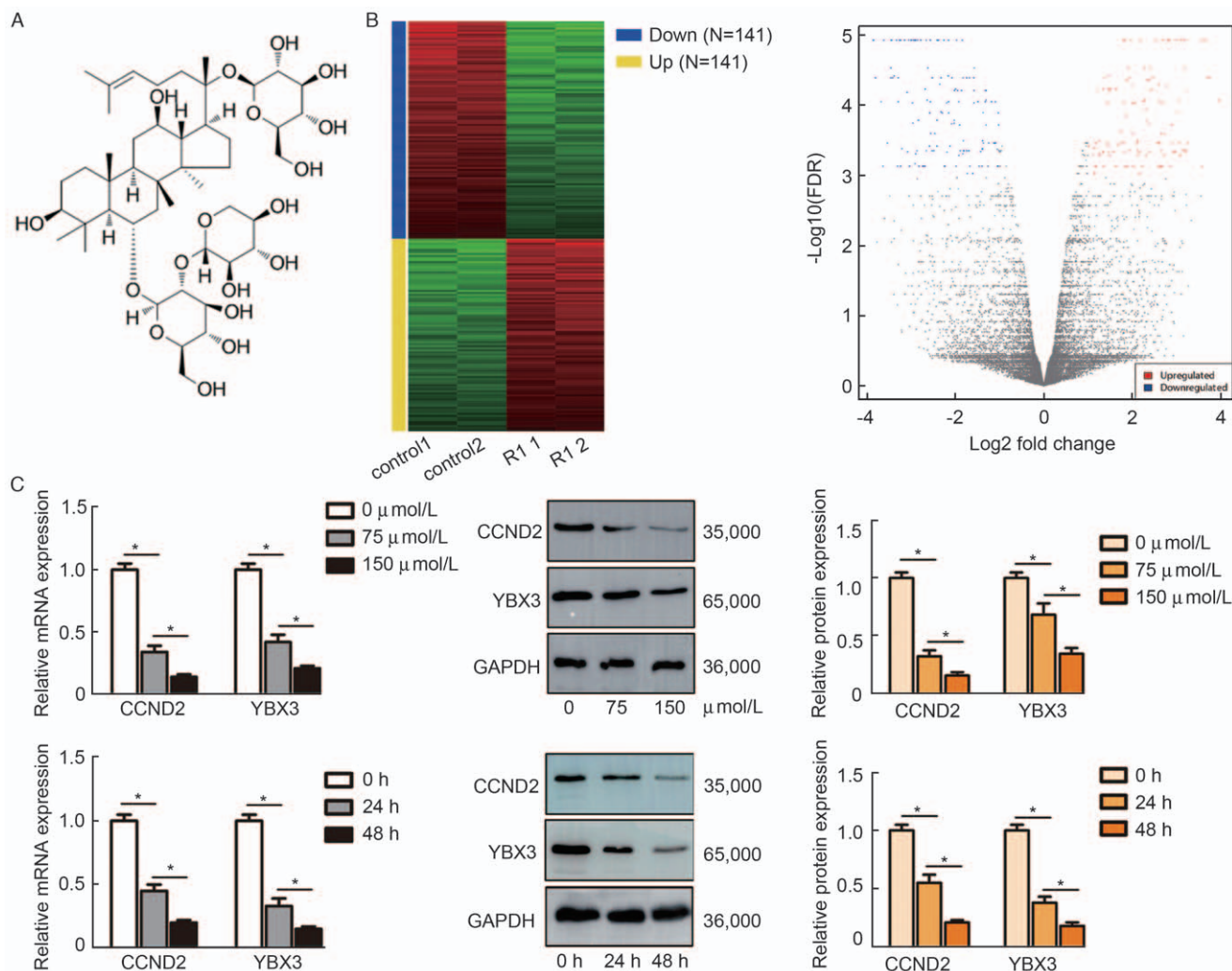


Figure 1: Identification of notoginsenoside R1 targets in MCF-7 cells. (A) The chemical structure of notoginsenoside R1. (B) Differentially expressed genes were detected using the GEO database (GES85871). (C) R1 treatment significantly decreased the expression of CCND2 and YBX3 in MCF-7 cells in a dose- and time-dependent manner. **P*<0.05.

Table 1: Top ten down-regulated genes were elucidated by GSE85871.

ID	P value	t	B	logFC	Gene.symbol	Gene.title
205804_s_at	0.0002372	-19.03	0.66188	-3.431	TRAF3IP3	TRAF3 interacting protein 3
220489_s_at	0.0004291	-15.73	0.42691	-3.448	SERINC2	Serine incorporator 2
206841_at	0.0007268	-13.28	0.16337	-3.451	PDE6H	Phosphodiesterase 6H
206433_s_at	0.0009893	-12.02	-0.01652	-3.451	SPOCK3	Sparc/osteonectin (testican) 3
215500_at	0.0032183	-8.18	-0.88305	-3.534	SNX29	Sorting nexin 29
205587_at	0.0006082	-14.06	0.25858	-3.617	FGFR1OP	FGFR1 oncogene partner
213319_s_at	0.0019963	-9.56	-0.49887	-3.676	YBX3	Y-box binding protein 3
200953_s_at	0.0009744	-12.08	-0.00722	-3.802	CCND2	Cyclin D2
207930_at	0.0004448	-15.55	0.41069	-3.838	LCN1	Lipocalin 1
211617_at	0.0001866	-20.55	0.74019	-3.854	ALDOAP2	Aldolase, fructose-bisphosphate A pseudogene 2

Results

NGR1 treatment inhibits the expression of CCND2 and YBX3

The chemical structure of NGR1 is shown in Figure 1A (Based on <https://www.medchemexpress.cn/Notoginsenoside-R1.html?src=bd-product>). To investigate the impact of NGR1 treatment on BC genetic alterations, we screened the GEO database (GSE85871) and found that 141 genes were downregulated and 114 genes were upregulated in the treatment group compared with the control group [Figure 1B]. The top ten down-regulated genes after NGR1 treatment in BC cells are shown in Table 1. Western blotting and quantitative real time polymerase chain reaction tests were used to verify the results of the GEO analysis. As shown in Figure 1C, there were clear trends of decreasing expression of CCND2 and YBX3 proteins in BC cells with NGR1 treatment in both dose- and time-dependent manners ($F = 441.1$, $P < 0.0001$). Together, these results indicated that treatment with NGR1 exerts an obvious inhibitory effect on the expression of CCND2 and YBX3 in BC cells. In addition, both CCND2 and YBX3 are oncogenes in many kinds of cancers, and it can be speculated that NGR1 exerts a cancer suppressive effect by down-regulating the expression of multiple oncogenes.

NGR1 treatment inhibits the migration, invasion, and angiogenesis of MCF-7 and MDA-MB-231 cells

Two sets of assays examined the impact of NGR1 on the proliferation of MCF-7 and MDA-MB-231 cells with different NGR1 doses and different exposure times. BC cells were treated with different concentrations of NGR1 for 24, 48, and 72 h, and cell counting kit-8 assays were then performed. The results are shown in Figure 2A. With the increase in the dose or the prolonged action of NGR1, the cell proliferation ability decreased rapidly. The 50% growth inhibitory concentration for MCF-7 cells at 24 h was 148.9 $\mu\text{mol/L}$. Colony formation assays were performed to analyze the long-term effect of NGR1 treatment on the proliferation of MCF-7 and MDA-MB-231 cells. The results indicated the same conclusion that NGR1 inhibited the proliferation ability of BC cells [Figure 2B] ($F = 62.2$, $P < 0.0001$). To evaluate whether NGR1 affects cell migration, invasion, and angiogenesis ability, Transwell assays with and without Matrigel and capillary tube formation assays were performed. The

results shown in Figure 2C and 2D show that NGR1 treatment obviously weakened the BC cell migration, invasion, and angiogenesis abilities as the dose increased. Collectively, these data suggest that NGR1 treatment can attenuate BC progression *in vitro* by altering proliferation, migration, invasion, and angiogenesis.

NGR1 regulates the cell cycle and apoptosis in MCF-7 cells

To assess the influence of NGR1 on the cell cycle, flow cytometry was used. The proportions of MCF-7 cells arrested in the G1 phase were 36.94% \pm 6.78%, 45.06% \pm 5.60%, and 59.46% \pm 5.60% in the control group, 75, and 150 $\mu\text{mol/L}$ groups, respectively [Figure 3A]. To evaluate the possible mechanism of apoptosis induced by NGR1, the main proteins of the mitochondrial pathway were examined by western blotting. The results showed that NGR1 induced an increase in the protein levels of Bax, cleaved caspase-3, and cleaved caspase-9 [Figure 3B]. Apoptotic MCF-7 cells were also detected by TUNEL staining after treatment with NGR1. All of the nuclei were stained blue by 4,6-diamino-2-phenyl indole, while apoptotic nuclei were stained green in the TUNEL assays [Figure 3C]. Significant changes were detected between groups, and a higher percentage of apoptosis events occurred in the NGR1 high-dose group compared with the low-dose group and control group.

NGR1 inhibits the KRAS/PI3K/Akt pathway via YBX3

Previous results have demonstrated that NGR1 regulates the cell cycle by downregulating CCND2. Further experiments should focus on the molecular regulatory mechanism of YBX3 in BC. To study the further regulatory mechanism of YBX3 in MCF-7 cells, we performed a ChIP-seq to the YBX3 gene in MCF-7 cells. A pie chart was generated to illustrate how peaks were distributed over important genomic features [Figure 4A]. Motif centrality analysis of YBX3 binding regions was performed using CentriMo [Figure 4B]. Kyoto Encyclopedia of Genes and Genomes (KEGG) pathway enrichment analysis of YBX3 ChIP-seq promoters with the top five enrichment scores is shown in Figure 4C; the PI3K/Akt pathway was the most enriched. Thus, YBX3 might up-regulate the PI3K/Akt pathway, and ChIP experiments verified that YBX3 plays such a role by binding the promoter regions of KRAS [Figure 4D]. Quantitative real time polymerase chain

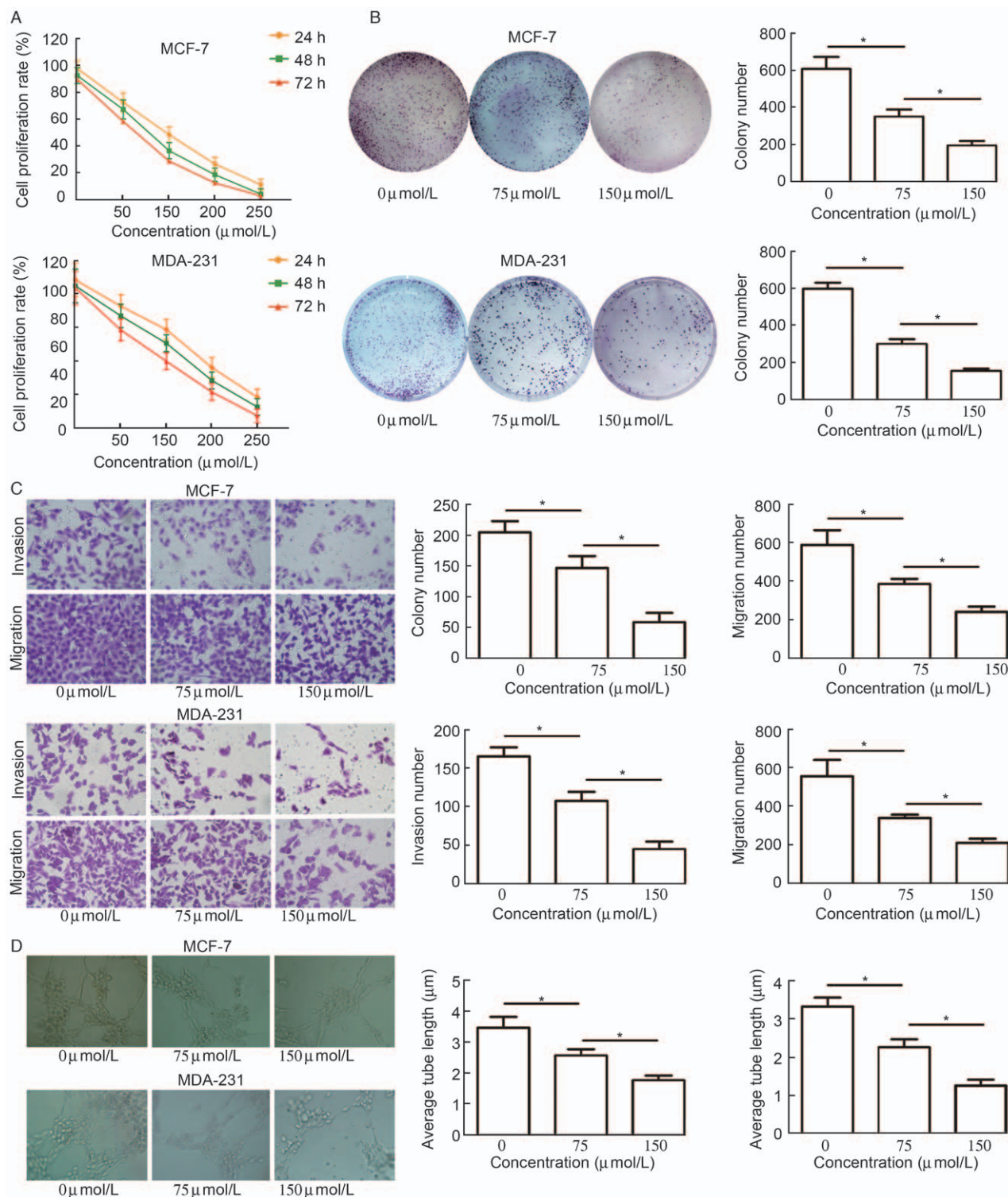


Figure 2: Notoginsenoside R1 suppresses the proliferation, migration, invasiveness, and angiogenic capacity of BC cells. (A) BC cells after treatment with R1 (0, 50, 100, 150, or 200 $\mu\text{mol/L}$) for 24, 48, or 72 h. R1 suppressed the proliferation of breast cancer cells in a dose- and time-dependent manner. (B) Photomicrographs of crystal violet-stained colonies of BC cells growing in six-well plates for 7 days after R1 treatment. R1 inhibited colony formation in a breast cancer cell line in a dose-dependent manner. (C) The cells were treated with R1 for 24 h. The images show that R1 inhibited the invasion and migration of MCF-7 cells across the Transwell inserts ($F=62.2, P<0.0001$). (D) Capillary tube formation (CTF) assays. All data represent the mean \pm standard error of the mean of values from three biological replicates ($F=80.11, P<0.0001$). * $P<0.05$. BC: Breast cancer.

reaction also demonstrated that the expression of KRAS was regulated by YBX3 [Figure 4E]. To connect the above conclusions to form an axis, we performed western blotting assays which indicated that NGR1 inhibited the

KRAS/PI3K/Akt pathway by decreasing YBX3 [Figure 4F]. It was shown that P-PI3K and P-AKT, the key proteins in the PI3K/Akt pathway, were down-regulated with increasing NGR1 concentration. Meanwhile, the expression of

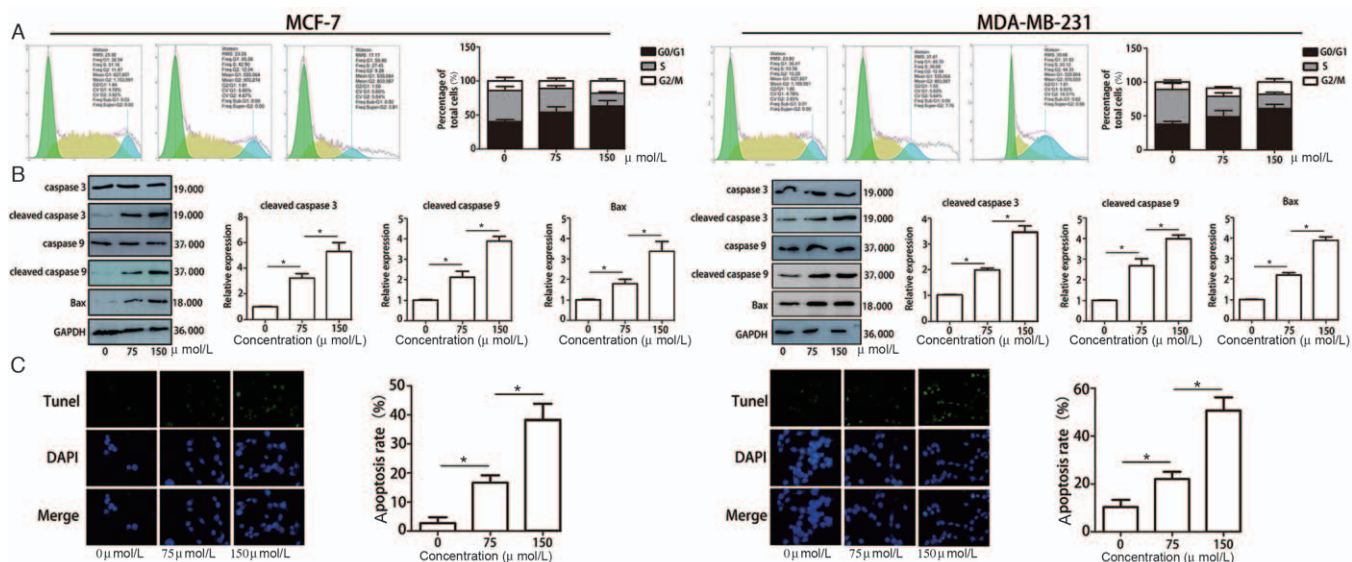


Figure 3: Notoginsenoside R1 regulates the MCF-7 cell cycle and apoptosis. (A) FACS analysis showing significant decreases in MCF-7 and MDA-MB-231 cells in the S phase after notoginsenoside R1 treatment ($F = 90.66$, $P < 0.0001$). (B, C) The effect of notoginsenoside R1 on cell apoptosis was measured by TUNEL and Western blotting assays. The error bars in all graphs represent SD, and each experiment was repeated three times ($F = 70.89$, $P < 0.0001$). * $P < 0.05$. SD: Standard deviation.

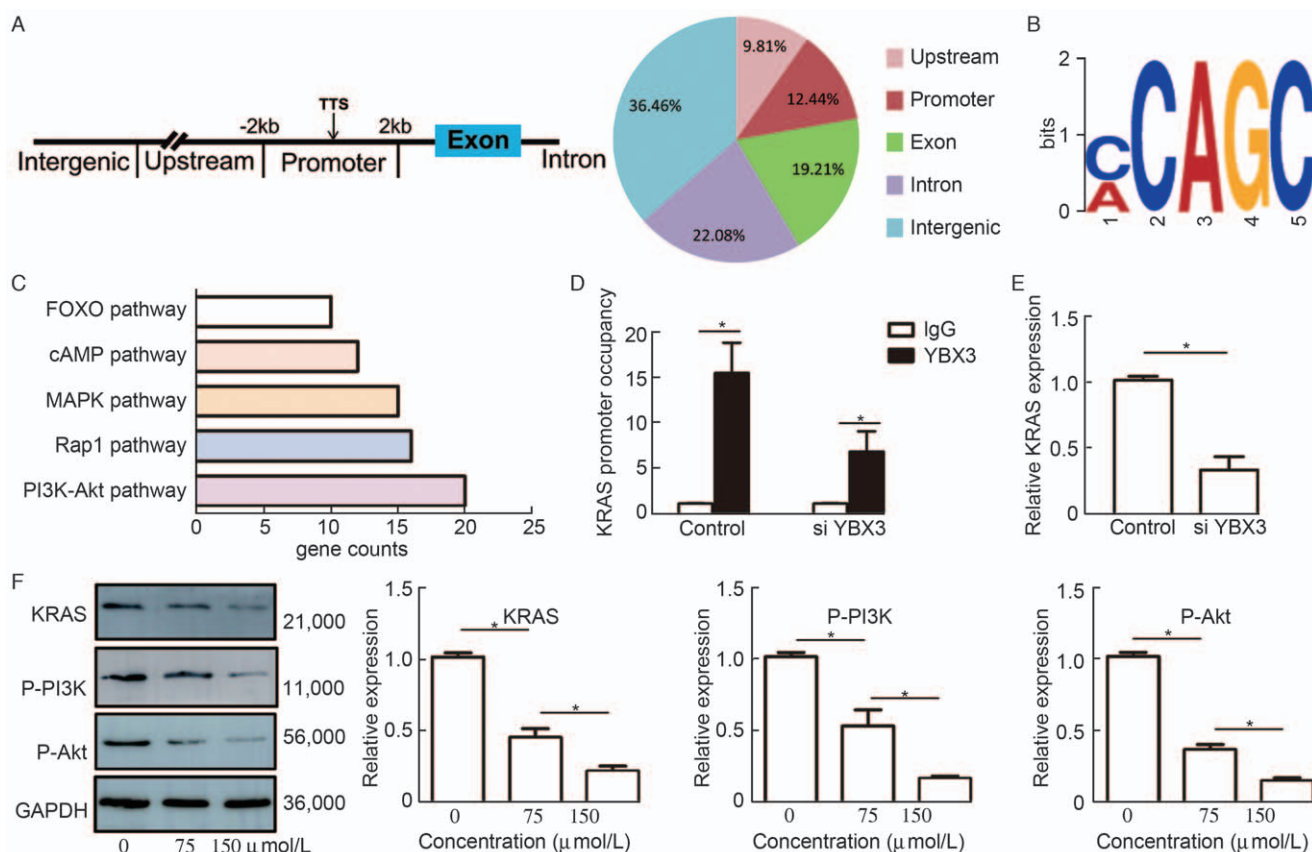


Figure 4: Notoginsenoside R1 inhibits the KRAS/PI3K/Akt pathway via YBX3. (A) Pie diagram illustrates how peaks are distributed over important genomic features. (B) Motif centrality analysis of YBX3 binding regions was performed using CentriMo. (C) KEGG pathway enrichment analysis of YBX3 ChIP-seq promoters with the top five enrichment scores. (D) The ChIP assay results confirmed the occupancy of YBX3 in the KRAS promoter ($F = 75.36$, $P < 0.0001$). (E) The expression of KRAS was down-regulated after siYBX3 transfection. (F) The expression of KRAS/p-PI3K/p-Akt was measured by Western blotting after notoginsenoside R1 treatment. ChIP-seq: Chromatin immunoprecipitation-seq; KEGG: Kyoto Encyclopedia of Genes and Genomes * $P < 0.001$.

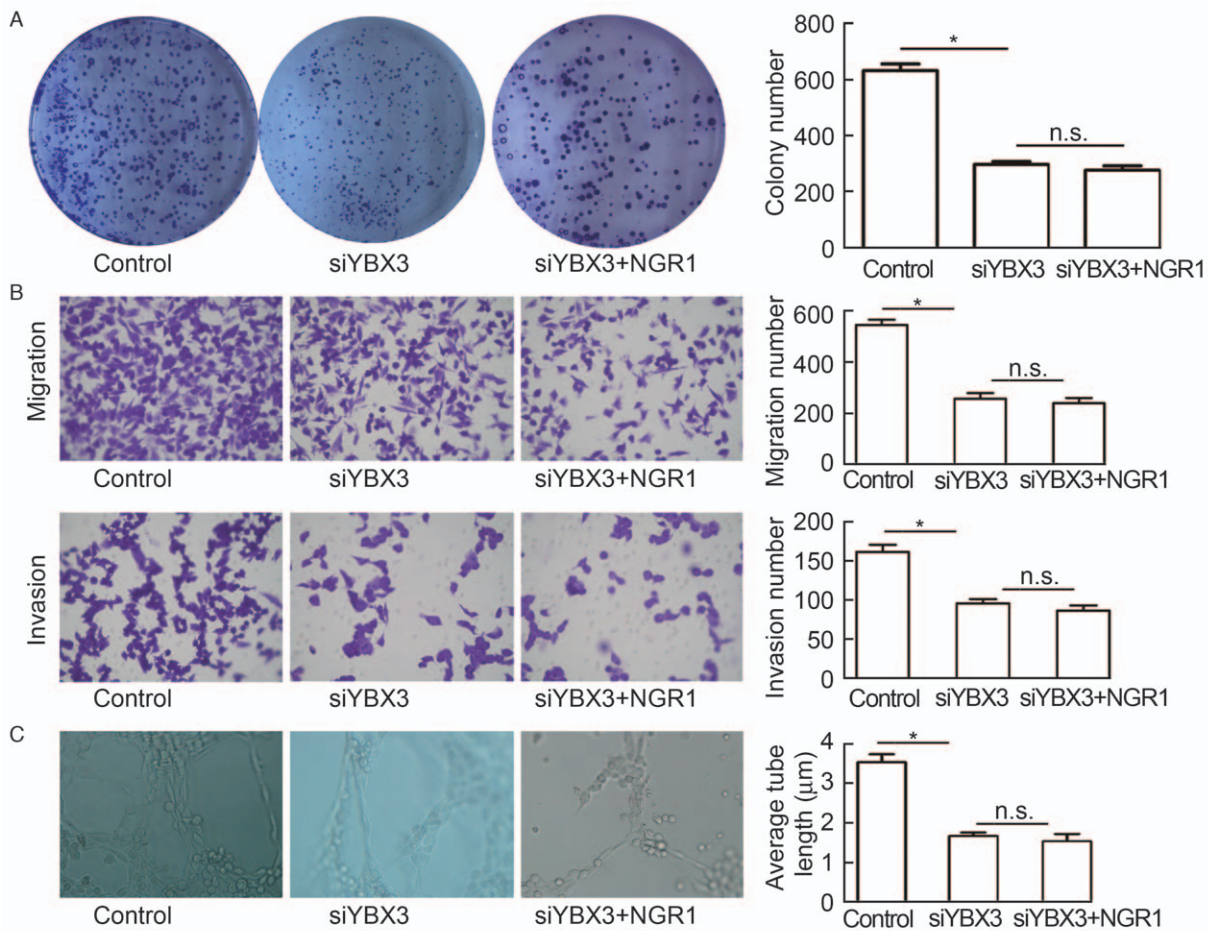


Figure 5: Notoginsenoside R1 inhibits BC aggressiveness by targeting YBX3. Colony formation (A), Transwell (B), and tube formation assays (C) were used to detect the effect of NGR1 on BC cells after YBX3 knockdown. Cells were stained with 0.1% crystal violet (original magnification $\times 400$). BC: Breast cancer. * $P < 0.001$. n.s.: Not significant.

KRAS was also suppressed by NGR1 treatment. Furthermore, cell functional experiments were performed to detect the effect of NGR1 on BC cells after YBX3 knockdown, such as colony formation and Transwell assays [Figure 5A–C]. The results showed NGR1 had little impact on BC cells after YBX3 knockdown, which means NGR1 could regulate BC progression by targeting YBX3 directly.

Discussion

In this study, we demonstrated that treatment with NGR1 significantly attenuated the growth of MCF-7 and MDA-MB-231 cells in a dose- and time-dependent manner. Next, we examined the effect of NGR1 on tumor-promoting activities including proliferation, invasion, and angiogenesis. As expected, NGR1 played a significant role in suppressing the tumorigenesis of MCF-7 and MDA-MB-231 cells *in vitro*. Additionally, NGR1 treatment induced cell cycle arrest and apoptosis in MCF-7 cells via the KRAS/PI3K/Akt pathway. Furthermore, the data from the sequencing models of the control group and NGR1-treated

group revealed the genes specifically downregulated by NGR1 treatment. Western blotting also indicated the down-regulation of *CCND2* and *YBX3* by NGR1 treatment in a dose- and time-dependent manner in MCF-7 cells. Thus, we illustrated that NGR1 may affect the growth or progression of MCF-7 cells by changing the expression of the *CCND2* and *YBX3* genes. Furthermore, KEGG enrichment analysis showed that the PI3K/Akt pathway was the pathway most closely related to *YBX3* in MCF-7 cells. ChIP assays further demonstrated that *YBX3* activated the PI3K/Akt pathway by combining it with KRAS. Consequently, these findings indicated an anti-cancer role of NGR1 in MCF-7 cells and revealed a potential molecular mechanism by which the *YBX3*/KRAS/PI3K/Akt axis functions in MCF-7 cells, as its inhibition has been associated with proliferation, migration, invasion, and angiogenesis in MCF-7 cells.

The main components of *P. notoginseng* are saponins. Additionally, three major types of saponins in *P. notoginseng* are ginsenosides (eg, Rb1, Rg1, Rg3), notoginsenosides (eg, R1, R2, R3), and jiaogulan glucosides (eg, R6). NGR1 is the most abundant notoginseno-

side in *P. notoginseng*.^[26,27] Previous anti-cancer studies have indicated that ginsenosides Rb1 suppresses phorbol myristate acetate-induced invasion and migration in MCF-7 cells.^[28] However, we are the first to report that NGR1 significantly suppresses BC metastasis and to clarify its molecular mechanisms in MCF-7 cells. Moreover, our results are consistent with those observed in other human malignancies, such as colon cancer and liver cancer.^[29,30] One of the related findings is that NGR1 inhibits the migration, invasion, and adhesion of HCT-116 cells^[13] by regulating MMP-9, integrin-1, E-selectin, and intercellular cell adhesion molecule-1 expression. Moreover, ginsenoside Rg1 also suppresses transforming growth factor β 1-induced invasion and migration in HepG2 liver cancer cells.^[30] The above studies indicate that saponins can reduce the tumorigenesis of many kinds of cancers. However, the effect of NGR1 on BC has not been studied. We are the first to show that NGR1 inhibits the tumorigenesis of MCF-7 cells and promotes cell cycle arrest and apoptosis of MCF-7 cells.

The *YBX3* gene is located on chromosome 12 at locus p13.1 and encodes two spliced mRNA isoforms, which act as tumor promoters.^[12,20-22,31] *CCND2* is another tumor promoter that plays a significant role in accelerating cell growth and cell migration, yet the inhibition of *CCND2* triggers cell apoptosis.^[23-25] In this study, we demonstrated that NGR1 treatment causes a decrease in the expression of *CCND2* in a time- and dose-dependent manner in MCF-7 cells. However, the detailed mechanism of *CCND2* in BC was not explored in this study. However, it is clear that *CCND2*, an oncogene in many cancers, plays a role in MCF-7 cells. On the other hand, we clarified the mechanisms of *YBX3* in MCF-7 cells. With ChIP-seq analysis, KEGG pathway analysis, and other detection methods, we predicted and verified the mechanism of *YBX3* in MCF-7 cells. This is the first report that *YBX3* works by combining with *KRAS* to activate the PI3K/Akt signaling pathway, and *KRAS* is an established activator of the PI3K/Akt signaling pathway.

Funding

This work was supported by grants from the National Natural Science Foundation of China (No. 81260576), the Major Program of Science and Technology Foundation of Guizhou Province (QKHJZ[2014]2003), the Major Science and Technology Projects of Guizhou Province (QKHJZ[2015]2002-2-5), and the Science and Technology Foundation of Guizhou Province (QKHJY[2011]3007).

Conflicts of interest

None.

References

- Kumar M, Salem K, Tevaarwerk AJ, Strigel RM, Fowler AM. Recent advances in imaging steroid hormone receptors in breast cancer. *J Nucl Med* 2020;61:172–176. doi: 10.2967/jnumed.119.228858.
- Narod SA. Breast cancer in young women. *Nat Rev Clin Oncol* 2012;9:460–470. doi: 10.1038/nrclinonc.2012.102.
- Garrido-Castro AC, Lin NU, Polyak K. Insights into molecular classifications of triple-negative breast cancer: improving patient selection for treatment. *Cancer Discov* 2019;9:176–198. doi: 10.1158/2159-8290.CD-18-1177.
- Thakur V, Kutty RV. Recent advances in nanotheranostics for triple negative breast cancer treatment. *J Exp Clin Cancer Res* 2019;38:430. doi: 10.1186/s13046-019-1443-1.
- Castaneda SA, Strasser J. Updates in the treatment of breast cancer with radiotherapy. *Surg Oncol Clin N Am* 2017;26:371–382. doi: 10.1016/j.soc.2017.01.013.
- Ferlay J, Colombet M, Soerjomataram I, Mathers C, Parkin DM, Pineros M, et al. Estimating the global cancer incidence and mortality in 2018: GLOBOCAN sources and methods. *Int J Cancer* 2019;144:1941–1953. doi: 10.1002/ijc.31937.
- Tagliafico AS, Piana M, Schenone D, Lai R, Massone AM, Houssami N. Overview of radiomics in breast cancer diagnosis and prognostication. *Breast* 2019;49:74–80. doi: 10.1016/j.breast.2019.10.018.
- Li H, Deng CQ, Chen BY, Zhang SP, Liang Y, Luo XG. Total saponins of *Panax notoginseng* modulate the expression of caspases and attenuate apoptosis in rats following focal cerebral ischemia-reperfusion. *J Ethnopharmacol* 2009;121:412–418. doi: 10.1016/j.jep.2008.10.042.
- Meng X, Sun G, Ye J, Xu H, Wang H, Sun X. Notoginsenoside R1-mediated neuroprotection involves estrogen receptor-dependent crosstalk between Akt and ERK1/2 pathways: a novel mechanism of Nrf2/ARE signaling activation. *Free Radic Res* 2014;48:445–460. doi: 10.3109/10715762.2014.885117.
- Pan C, Huo Y, An X, Singh G, Chen M, Yang Z, et al. *Panax notoginseng* and its components decreased hypertension via stimulation of endothelial-dependent vessel dilatation. *Vascu Pharmacol* 2012;56:150–158. doi: 10.1016/j.vph.2011.12.006.
- Sun K, Wang CS, Guo J, Horie Y, Fang SP, Wang F, et al. Protective effects of ginsenoside Rb1, ginsenoside Rg1, and notoginsenoside R1 on lipopolysaccharide-induced microcirculatory disturbance in rat mesentery. *Life Sci* 2007;81:509–518. doi: 10.1016/j.lfs.2007.06.008.
- Wang W, Zhang X, Qin JJ, Voruganti S, Nag SA, Wang MH, et al. Natural product ginsenoside 25-OCH₃-PPD inhibits breast cancer growth and metastasis through down-regulating MDM2. *PLoS One* 2012;7:e41586. doi: 10.1371/journal.pone.0041586.
- Lee CY, Hsieh SL, Hsieh S, Tsai CC, Hsieh LC, Kuo YH, et al. Inhibition of human colorectal cancer metastasis by notoginsenoside R1, an important compound from *Panax notoginseng*. *Oncol Rep* 2017;37:399–407. doi: 10.3892/or.2016.5222.
- Yu Y, Sun G, Luo Y, Wang M, Chen R, Zhang J, et al. Cardioprotective effects of Notoginsenoside R1 against ischemia/reperfusion injuries by regulating oxidative stress- and endoplasmic reticulum stress-related signaling pathways. *Sci Rep* 2016;6:21730. doi: 10.1038/srep21730.
- Zhang HS, Wang SQ. Notoginsenoside R1 inhibits TNF- α -induced fibronectin production in smooth muscle cells via the ROS/ERK pathway. *Free Radic Biol Med* 2006;40:1664–1674. doi: 10.1016/j.freeradbiomed.2006.01.003.
- Zhou N, Tang Y, Keep RF, Ma X, Xiang J. Antioxidative effects of *Panax notoginseng* saponins in brain cells. *Phytomedicine* 2014;21:1189–1195. doi: 10.1016/j.phymed.2014.05.004.
- Evan GI, Vousden KH. Proliferation, cell cycle and apoptosis in cancer. *Nature* 2001;411:342–348. doi: 10.1038/35077213.
- Mohammad RM, Muqbil I, Lowe L, Yedjou C, Hsu HY, Lin LT, et al. Broad targeting of resistance to apoptosis in cancer. *Semin Cancer Biol* 2015;35:S78–S103. doi: 10.1016/j.semcancer.2015.03.001.
- Ouyang L, Shi Z, Zhao S, Wang FT, Zhou TT, Liu B, et al. Programmed cell death pathways in cancer: a review of apoptosis, autophagy and programmed necrosis. *Cell Prolif* 2012;45:487–498. doi: 10.1111/j.1365-2184.2012.00845.x.
- Ladomery M, Sommerville J. A role for Y-box proteins in cell proliferation. *Bioessays* 1995;17:9–11. doi: 10.1002/bies.950170104.
- Yasen M, Kajino K, Kano S, Tobita H, Yamamoto J, Uchiumi T, et al. The up-regulation of Y-box binding proteins (DNA binding protein A and Y-box binding protein-1) as prognostic markers of hepatocellular carcinoma. *Clin Cancer Res* 2005;11:7354–7361. doi: 10.1158/1078-0432.CCR-05-1027.
- Yasen M, Obulhasim G, Kajino K, Mogushi K, Mizushima H, Tanaka S, et al. DNA binding protein A expression and methylation status in hepatocellular carcinoma and the adjacent tissue. *Int J Oncol* 2012;40:789–797. doi: 10.3892/ijo.2011.1282.

23. Canavese M, Santo L, Raje N. Cyclin dependent kinases in cancer: potential for therapeutic intervention. *Cancer Biol Ther* 2012; 13:451–457. doi: 10.4161/cbt.19589.
24. Jia M, Li X, Jiang C, Wang K, Zuo T, He G, *et al.* Testis-enriched circular RNA circ-Bbs9 plays an important role in Leydig cell proliferation by regulating a CyclinD2-dependent pathway. *Reprod Fertil Dev* 2020;32:355–362. doi: 10.1071/RD18474.
25. Li WC, Wu YQ, Gao B, Wang CY, Zhang JJ. MiRNA-574-3p inhibits cell progression by directly targeting CCND2 in colorectal cancer. *Biosci Rep* 2019;39:BSR20190976. doi: 10.1042/BSR20190976.
26. Yang X, Xiong X, Wang H, Wang J. Protective effects of Panax notoginseng saponins on cardiovascular diseases: a comprehensive overview of experimental studies. *Evid Based Complement Alternat Med* 2014;2014:204840. doi: 10.1155/2014/204840.
27. Jiang R, Dong J, Li X, Du F, Jia W, Xu F, *et al.* Molecular mechanisms governing different pharmacokinetics of ginsenosides and potential for ginsenoside-perpetrated herb-drug interactions on OATP1B3. *Br J Pharmacol* 2015;172:1059–1073. doi: 10.1111/bph.12971.
28. Li L, Wang Y, Qi B, Yuan D, Dong S, Guo D, *et al.* Suppression of PMA-induced tumor cell invasion and migration by ginsenoside Rg1 via the inhibition of NF-kappaB-dependent MMP-9 expression. *Oncol Rep* 2014;32:1779–1786. doi: 10.3892/or.2014.3422.
29. Lee SG, Kang YJ, Nam JO. Anti-metastasis effects of ginsenoside Rg3 in B16F10 cells. *J Microbiol Biotechnol* 2015;25:1997–2006. doi: 10.4014/jmb.1506.06002.
30. Yu M, Yu X, Guo D, Yu B, Li L, Liao Q, *et al.* Ginsenoside Rg1 attenuates invasion and migration by inhibiting transforming growth factor-beta1-induced epithelial to mesenchymal transition in HepG2 cells. *Mol Med Rep* 2015;11:3167–3173. doi: 10.3892/mmr.2014.3098.
31. Wolffe AP. Structural and functional properties of the evolutionarily ancient Y-box family of nucleic acid binding proteins. *Bioessays* 1994;16:245–251. doi: 10.1002/bies.950160407.

How to cite this article: Qin HL, Wang XJ, Yang BX, Du B, Yun XL. Notoginsenoside R1 attenuates breast cancer progression by targeting CCND2 and YBX3. *Chin Med J* 2021;134:546–554. doi: 10.1097/CM9.0000000000001328